Electronic Supplementary Material (ESI) for Journal of Materials Chemistry A.

Electronic Supporting Information (ESI) for the manuscript:

Tuning the Selectivity of Light Hydrocarbons in Natural Gas in a Family of Isoreticular MOFs

Thais Grancha, Marta Mon, Jesús Ferrando-Soria,* Jorge Gascon, Beatriz Seoane, Enrique V. Ramos-Fernandez, Donatella Armentano,* and Emilio Pardo*

Experimental Section

Materials. All chemicals were of reagent grade quality. They were purchased from commercial sources and used as received. **{$Ca^{II}Cu^{II}_6$[(S,S)-alamox]$_3$(OH)$_2$(H_2O)} · 32H_2O (1)** was prepared as reported previously.[1]

HMeEt-(S,S)-valmox and HMeEt-(S,S)-leumox: Both proligands were obtained, separately, following the same synthetic procedure. The hydrochloride esters of L-Valine or L-Leucine (60.0 mmol) were dissolved in dichloromethane solutions (200 mL) and charged with triethylamine (16.7 mL, 120.0 mmol). To the resulting colourless reaction mixtures, solutions containing oxalyl chloride (2.58 mL, 30.0 mmol) in dichloromethane (200 mL) were added dropwise under vigorous stirring at 0 °C on an ice-bath. After further stirring during one hour, the small amount of white solid (Et_3NHCl) formed was filtered off and the resulting colourless solutions were then concentrated in a rotatory evaporator to a final volume of 100 mL. The resulting solutions were washed three times with water (3x50 mL) and finally, the solvent was removed in a rotatory evaporator to afford white solids which were collected with diethyl ether and dried under vacuum. **HMeEt-(S,S)-valmox:** Yield: 16.89 g, 89%; Anal. calcd (%) for $C_{14}H_{24}N_2O_6$ (316.3): C 53.15, H 7.65, N 8.86; found: C 53.12, H 7.39, N 8.89; ^{1}H NMR ([D_6]DMSO): 0.88 (dd, 6H; 2CH_3),2.22 (m, 2H, 2CH from –$CH(CH_3)_2$, 3.66 (s, 6H; 2CH_3 from –OCH_3), 4.15 (dd, 2H; 2CH), 8.74 (d, 2H; 2NH); IR (KBr): ν = 2980 and 2933 cm^{-1} (C-H), 1712 and 1621 cm^{-1} (C=O). **HMeEt-(S,S)-leumox:** Yield: 19.2 g, 93%; Anal. calcd (%) for $C_{10}H_{16}N_2O_6$ (344.4): C 55.80, H 8.19, N 8.13; found: C 55.73, H 8.01, N 8.15; ^{1}H NMR ([D_6]DMSO): 0.85 (m, 12H; 4CH_3 from 2 –$CH_2CH(CH_3)_2$), 1.55 (dd, 4H, 2CH_2 from 2 –$CH_2CH(CH_3)_2$), 1.80 (m, 2H, 2CH from 2 –$CH_2CH(CH_3)_2$), 3.62 (s, 6H; 2CH_3 from –OCH_3), 4.35 (m, 2H; 2CH), 9.02 (d, 2H; 2NH); IR (KBr): ν = 2986 and 2939 cm^{-1} (C-H), 1709 and 1621 cm^{-1} (C=O).

(Me_4N)$_2${Cu_2[(S,S)-valmox](OH)$_2$} · 2H_2O: HMeEt-(S,S)-valmox (9.49 g, 30 mmol) and HMeEt-(S,S)-leumox (10.33 g, 30 mmol), were suspended in methanol and water (50 mL), respectively, and treated with 25% methanolic solutions of Me_4NOH (36 mL,

[1] T. Grancha, J. Ferrando-Soria, J. Cano, P. Amorós, B. Seoane, J. Gascon, M. Bazaga-García, E. R. Losilla, A. Cabeza, D. Armentano and E. Pardo, *Chem. Mater.*, **2016**, *28*, 4608–4615.

12.5 mmol). Then, methanolic solutions (25 mL) of $CuCl_2$ (8.07 g, 60 mmol) were added dropwise under vigorous stirring. The resulting deep green solutions were filtered to remove solid particles and concentrated to a volume of *ca.* 20 mL in a rotary evaporator. The mixtures were then allowed to stand at 0 °C on an ice-bath for 30 min., and the resulting green polycrystalline solids were collected by filtration, gently washed with acetone and dried under vacuum. **$(Me_4N)_2\{Cu_2[(S,S)\text{-valmox}](OH)_2\} \cdot 2H_2O$**: Yield: 10.01 g, 53%; Anal. calcd for $C_{20}H_{46}Cu_2N_4O_{10}$ (629.7): C, 38.15; H, 7.36; N, 8.90%; Found: C, 38.13; H, 7.19; N, 8.95%; IR (KBr): ν = 3642 cm^{-1} (O-H), 2987 and 2932 cm^{-1} (C-H), 1712, 1643 and 1621 cm^{-1} (C=O). **$(Me_4N)_2\{Cu_2[(S,S)\text{-leumox}](OH)_2\} \cdot 2H_2O$**: Yield: 12.04 g, 61%; Anal. calcd for $C_{22}H_{50}Cu_2N_4O_{10}$ (657.7): C, 40.17; H, 7.66; N, 8.52%; Found: C, 40.01; H, 7.37; N, 8.61%; IR (KBr): ν = 3638 cm^{-1} (O-H), 2972 and 2931 cm^{-1} (C-H), 1710, 1651 and 1618 cm^{-1} (C=O).

Preparation of $\{Cu_6Ca[(S,S)\text{-valmox}]_3(OH)_2(H_2O)\} \cdot 13H_2O$ (2) and $\{Cu_6Ca[(S,S)\text{-leumox}]_3(OH)_2(H_2O)\} \cdot 11H_2O$ (3): Well-shaped hexagonal prisms of **2** and **3**, suitable for X-ray structural analysis, were obtained by slow diffusion, in H-shaped tubes, of 1:1 H_2O:CH_3OH solutions (v/v) of the corresponding dicopper(II) complex (0.18 mmol) in one arm and $CaCl_2$ (0.01 g, 0.06 mmol) in the other. Crystals appeared after several weeks. They were isolated by filtration on paper and air-dried.

Both compounds **2** and **3** can be alternatively obtained, in a multi-gram scale, by stirring stoichiometry amounts of $(Me_4N)_2\{Cu_2[(S,S)\text{-valmox}](OH)_2\} \cdot 2H_2O$ or $(Me_4N)_2\{Cu_2[(S,S)\text{-leumox}](OH)_2\} \cdot 2H_2O$ with $CaCl_2$ in water for 1 hour.

2: Yield: 77%; Anal. calcd for $C_{36}Cu_6CaH_{78}N_6O_{34}$ (1560.4): C, 27.71; H, 5.04; N, 5.39%; Found: C, 27.67; H, 5.01; N, 5.49%; IR (KBr): ν = 1606 cm^{-1} (C=O). **3:** Yield: 73%; Anal. calcd for $C_{42}Cu_6CaH_{86}N_6O_{32}$ (1608.5): C, 31.36; H, 5.39; N, 5.22%; Found: C, 31.22; H, 5.11; N, 5.23%; IR (KBr): ν = 1604 cm^{-1} (C=O).

Physical Techniques. Elemental (C, H, N) analyses were performed at the Microanalytical Service of the Universitat de València. ^{1}H NMR spectra were recorded at room temperature on a Bruker AC 200 (200.1 MHz) spectrometer. FT–IR spectra were recorded on a Perkin-Elmer 882 spectrophotometer as KBr pellets. Thermogravimetric analyses (TGA) data were recorded on an SDT-Q600 analyzer from TA instruments. The temperature varied from RT to 600 °C at a heating rate of 10

°C·min^{-1}. Measurements were carried out on samples in open platinum crucibles under a flow of air.

Gas adsorption. The N_2 and CO_2 adsorption-desorption isotherms at 77 K and 273 K, respectively, were carried out on policrystalline samples of **1-3** with a Micromeritics ASAP2020 instrument. Sample was first activated with methanol and then evacuated at 348 K during 16 hours under 10^{-6} Torr prior to their analysis. The Brunauer-Emmett-Teller (BET) surface area was calculated from the N_2 adsorption isotherm according to the criteria reported by Rouquerol *et al*. and de Lange *et al*.[2]

Hydrocarbon adsorption isotherms at 273K were performed in a home-made fully automated manometric equipment designed and constructed by the Advanced Materials Group (LMA), and now commercialized as N2GSorb-6 (Gas to Materials Technologies; www.g2mtech.com). Before the adsorption experiments, the samples were outgassed at 348 K for 16h under vacuum.

Kinetics of adsorption. Kinetic evaluation of the sorbents was performed at 273 K in glassmade manometric adsorption equipment using pure gas components. Prior to the adsorption experiment, the sample was degassed under vacuum at the activation temperature. The initial pressure in the manifold was defined at 750 mbar for all adsorbates. Once equilibrated, the manifold was expanded to the sample holder, pressure readings being recorded every second and lasting for ten minutes. The dead volume of the sample cell was measured by expansion of He from the manifold to the sample cell.

Breakthrough measurements. Breakthrough curve experiments for different mixtures of gases were carried out using a column at 298 K. The sample powder was packed in the middle part of the column. Here, the sample mass we used is 1.0 g. Breakthrough allows in situ activation of the sample under Helium flow. Mass flow controllers controlled the flow rates of all gases. Before the measurement, the sample was activated at the desired temperature for 19 hours. The gas stream from the outlet of the column was analyzed online with a mass spectrometer. In order to have into account the bed dispersion and its effect in the breakthrough curve shape, we used as internal

[2](a) Rouquerolt, J.; Avnir, D.; Fairbridge, C. W.; Everett, D. H.; Haynes, J. H.; Pernicone, N.; Ramsay, J. D. F.; Sing, K. S. W.; Unger, K. K. *Pure Appl. Chem.* **1994**, *66* (8), 1739. (b) De Lange, M. F.; Vlugt, T. J. H.; Gascon, J.; Kapteijn, F. *Microporous Mesoporous Mater.* **2014**, *200*, 199.

standard H_2. In others words, we co-feed a H_2 flow (H_2 is not adsorbed in this materials at this conditions) together with gases we want to separate. The amount of gas adsorbed was the difference between the shape of the CH_4 or C_2H_6 or C_3H_8 breakthrough and the H_2 breakthrough.

X-ray crystallographic data collection and structure refinement.

Selected crystal data for 1: $C_{36}Cu_6CaH_{78}N_6O_{34}$, hexagonal, space group $P6_3$, a = 17.783(3) Å, c = 12.889(2) Å, V = 3530(1) Å^3, T = 90(2) K, Z = 2, ρ_{calc} = 1.468 g.cm^{-3}, μ = 1.930 mm^{-1}, Flack parameter = 0.4(2), of the 20336 reflections collected, 4076 are unique and 1687 observed with $I > 2\sigma(I)$. Refinement of 128 parameters gave R = 0.0960 and R_w = 0.2383 for reflections with $I > 2\sigma(I)$ and R = 0.2290 and R_w = 0.3194 for all reflections, with S = 1.008. CCDC 1530549. Further detailed information of the structural data can be found at Table S1.

Selected crystal data for 2: $C_{42}Cu_6CaH_{86}N_6O_{32}$, hexagonal, space group $P6_3$, a = 17.603(6) Å, c = 13.045(4) Å, V = 3501(3) Å^3, T = 90(2) K, Z = 2, ρ_{calc} = 1.526 g.cm^{-3}, μ = 1.946 mm^{-1}, Flack parameter = 0.36(9), of the 47764 reflections collected, 4777 are unique and 2505 observed with $I > 2\sigma(I)$. Refinement of 179 parameters gave R = 0.0710 and R_w = 0.1810 for reflections with $I > 2\sigma(I)$ and R = 0.1175 and R_w = 0.2043 for all reflections, with S = 0.959. CCDC 1530550. Further detailed information of the structural data can be found at Table S1.

Suitable crystals (0.10 × 0.10 × 0.08 and 0.16 × 0.14 × 0.12 mm^3) were selected and mounted on a MITIGEN holder in Paratone oil and very quickly placed on a liquid nitrogen stream cooled at 90 K to avoid the possible degradation upon dehydration. Diffraction data were collected on a Bruker-Nonius X8APEXII CCD area detector diffractometer using graphite-monochromated Mo-K$_\alpha$ radiation (λ = 0.71073 Å). Due to the poor crystal quality, the diffraction patterns were affected by expected internal imperfections of the crystal that give, a high Rint value especially for **2** and a quite expected difficulty to perform a perfect correction of anisotropy (detected as Alerts A and B in the checkcifs). However, since the solution and refinement parameters are reasonable, we are confident that the crystal structure found is consistent. The data

were processed through the SAINT[3] reduction and SADABS[4] multi-scan absorption software. The structure was solved with the SHELXS structure solution program, using the Direct Methods solution method. The model was refined with version 2013/4 of SHELXL against F^2 on all data by full-matrix least squares.[5]

In sample **2**, to increase the data/parameters ratio, only the heavy atoms and some atoms of the coordinative core of the ligand in the Metal-Organic Frameworks were refined anisotropically whereas in **3** all non-hydrogen atoms were refined anisotropically except the carbon atoms of the flexible isobutyl chains and the oxygen atom of lattice water molecule. In both samples, **2** and **3**, the hydrogen atoms of the ligand, except for the hydroxo/water oxygen atom O(1H) (where the OH/H_2O statistic distribution is 2:1) were set in calculated positions and refined as riding atoms whereas those of the crystallization water molecules were neither found from ΔF map nor calculated.

The use of some C-C and C-N bond lengths restrains during the refinements [or the fixed positions for C(10) and C(9) as found from ΔF map in **2** and **3**, respectively] of the highly disordered carbon atoms of the isopropyl (**2**) and isobutyl (**3**) chains have been reasonable imposed and related to their extraordinary flexibility, these chains in fact are dynamic components of the frameworks. As a consequence Alerts A and B in the checkcifs, also related to short intra H···H, are detected. Furthermore, in **3**, a terminal $–CH_3$ group of an isobutyl chain [C(9)] is disordered being placed in special position and shared by three chains. It shows an occupancy factor of 0.333 imposed by symmetry reasons that accounts for the mismatch between the formula unit calculated and reported (levels Alert A in checkcifs).

The solvent molecules, even if not all the ones detected by TGA analysis in case of **3**, were located on a ΔF map but their oxygen atoms have a very large thermal motion because of the disorder [Alerts A in the CheckCIF], the quite large channels and the diffuse electron density related to the presence in the pores of highly flexible alkyl chains featured by this series of isoreticular MOFs likely account for that. As a

[3] SAINT, version 6.45, Bruker Analytical X-ray Systems, Madison, WI, 2003.
[4] Sheldrick G.M. SADABS Program for Absorption Correction, version 2.10, Analytical X-ray Systems, Madison, WI, 2003
[5] (a) G. M. Sheldrick, *Acta Cryst.* **2015**, *C71*, 3-8. (b) G. M. Sheldrick, *Acta Cryst.* **2008**, *A64*, 112-122. (c) SHELXTL-2013/4, Bruker Analytical X-ray Instruments, Madison, WI, 2013.

consequence, in **3** the contribution to the diffraction pattern from the highly disordered water molecules located in the voids that was not possible to find was subtracted from the observed data through the SQUEEZE method, implemented in PLATON.[4] The residual agreement factors for reflections with $I > 2\sigma(I)$ before SQUEEZE are $R = 0.0832$ and $R_w = 0.2323$, and after R1 = 0.0710, wR2 = 0.1810. The final formulation of the compound is in agreement with the residual electron density and volume.

A summary of the crystallographic data and structure refinement for the two compounds is given in Table S1.

In general all the Alerts A and B in the checkcifs, [except the two Alerts B concerning mismatches of Calculated and Reported Mol. Weight in **3**, related to the porous nature of the Metal Organic Frameworks for which not all the solvent molecules detected by TGA analysis, have been modeled] are related to both the intrinsic porous and flexible nature of the reported materials.

The final geometrical calculations on free voids and the graphical manipulations were carried out with PLATON[6] implemented in WinGX,[7] and CRYSTAL MAKER[8] programs, respectively.

X-ray Powder Diffraction Measurements. Polycrystalline samples of **1**-**3** were introduced into 0.5 mm borosilicate capillaries prior to being mounted and aligned on a Empyrean PANalytical powder diffractometer, using Cu Kα radiation (λ = 1.54056 Å). For each sample, five repeated measurements were collected at room temperature (2θ = 2–40°) and merged in a single diffractogram.

[6] Spek, A. L. *Acta Crystallogr. Sect. D, Biol. Crystallogr.* **2009**, *65*, 148.
[7] Farrugia, L. J. *J. Appl. Crystallogr.* **1999**, *32*, 837.
[8] D. Palmer, CRYSTAL MAKER, Cambridge University Technical Services, C. No Title, 1996.

Table S1. Crystal data and structure refinement for 2 and 3.

Compound	**2**	**3**
Formula	$C_{36}Cu_6CaH_{78}N_6O_{34}$	$C_{42}Cu_6CaH_{86}N_6O_{32}$
M (g mol^{-1})	1560.36	1608.48
λ (Å)	0.71073	0.71073
Crystal system	hexagonal	hexagonal
Space group	$P6_3$	$P6_3$
a (Å)	17.783(3)	17.603(6)
c (Å)	12.889(2)	13.045(4)
V (Å^3)	3530(1)	3501(3)
Z	2	2
ρ_{calc} (g cm^{-3})	1.468	1.526
μ (mm^{-1})	1.930	1.946
T (K)	90	90
θ range for data collection (°)	1.32 – 26.0	1.33 – 26.0
Completeness to θ = 25.0	100 %	100 %
Measured reflections	20336	47764
Unique reflections (Rint)	4076 (0.21)	4777 (0.10)
Observed reflections [$I > 2\sigma(I)$]	1687	2505
Goof	1.008	0.959
R^a [$I > 2\sigma(I)$] (all data)	0.0960 (0.2290)	0.0710 (0.1175)
wR^b [$I > 2\sigma(I)$] (all data)	0.2383 (0.3194)	0.1810 (0.2043)

[a] $R = \sum(|F_o| - |F_c|)/\sum|F_o|$. [b] $wR = [\sum w(|F_o| - |F_c|)^2/\sum w|F_o|^2]^{1/2}$.

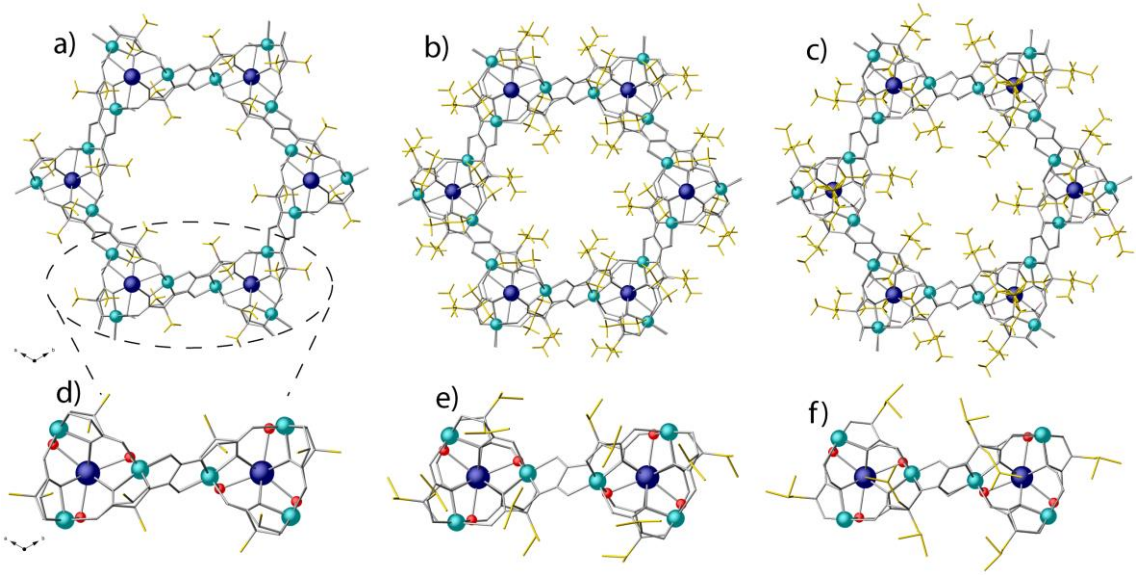

Figure S1. Projection view of one hexagonal channel of **1-3 (**a-c**)** along the crystallographic *c* axis showing the filling of the hexagonal pores by methyl (**1**), isopropyl (**2**) and isobutyl (**3**) groups. Details of a fragment of the building blocks dimers (d-f) where the oxygen atom of the μ_3 aqua/hydroxo group is depicted as red spheres. Copper and calcium atoms are represented by green and purple spheres, respectively, whereas the ligands are depicted as grey sticks except the amino acid residues depicted in yellow sticks. (carbon: gray, oxygen: red and nitrogen: blue).

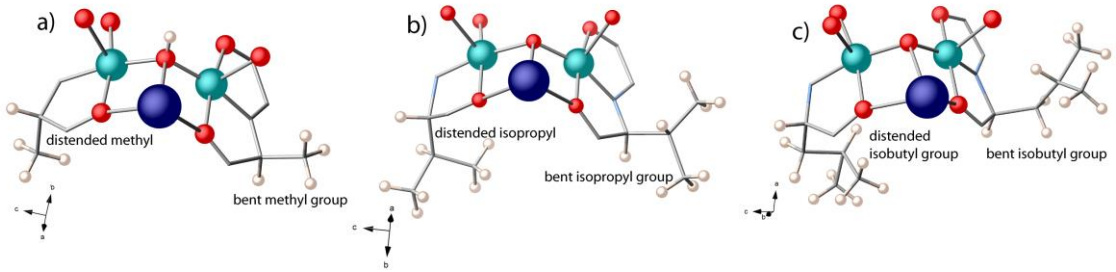

Figure S2. Lattice asymmetric units without crystallization solvent molecules of a) **1**, b) **2** and c) **3** evidently featuring highly flexible aminoacid residues side chains, which show different conformations of the hydrophobic methyl (**1**), isopropyl (**2**) and isobutyl (**3**) groups depending on the steric hindrance. Color scheme: Calcium(II) purple; copper(II), green; oxygen, red; nitrogen, light blue; hydrogen, white; carbon atoms have been depicted as grey sticks.

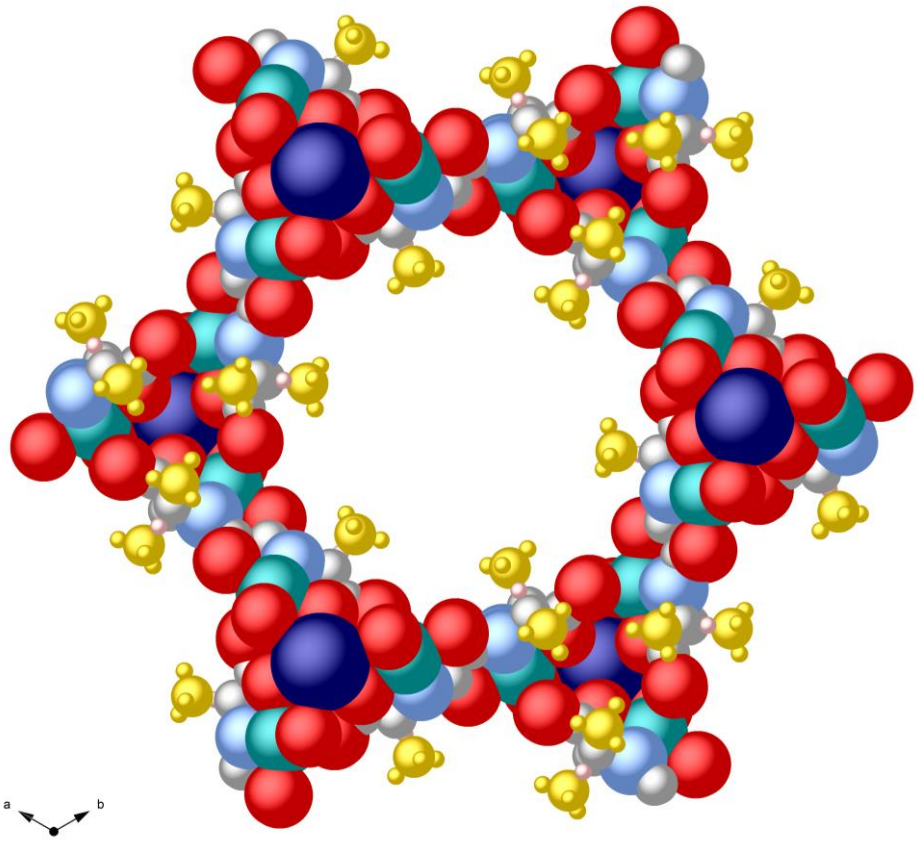

Figure S3. View along the *c* axis of one hexagonal pore of **1** using the space filling model (Van der Waals radii). Color scheme: Calcium(II) purple; copper(II), green; methyl group of alanine residue, yellow gold; nitrogen, light blue; oxygen, red; carbon, grey.

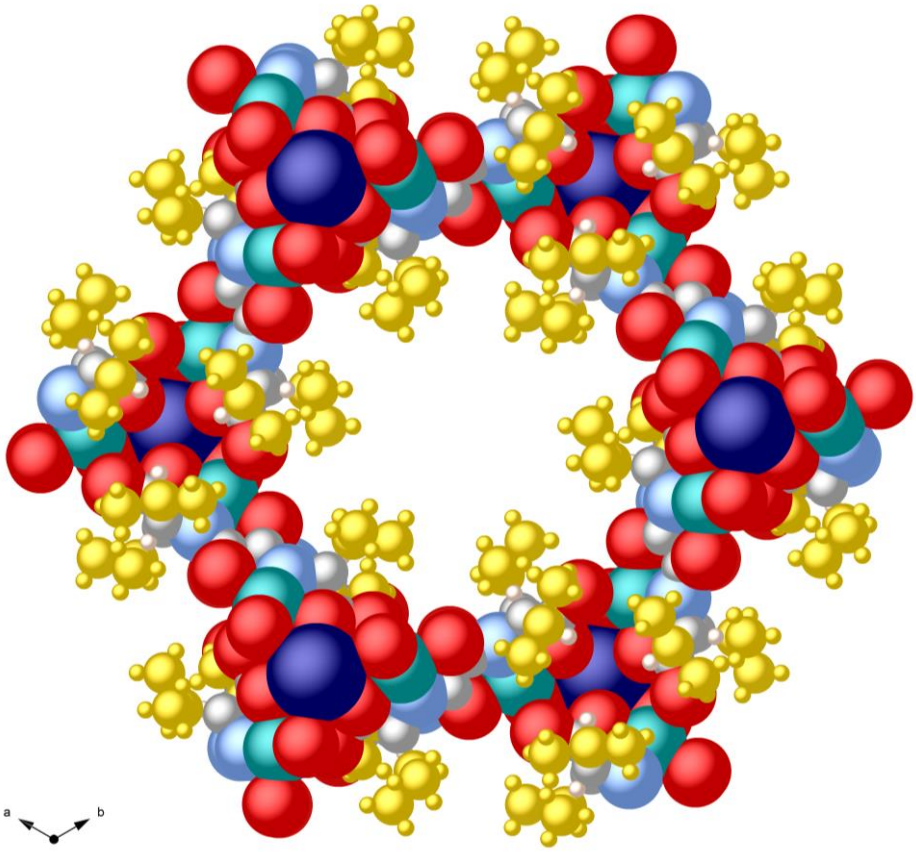

Figure S4. View along the *c* axis of one hexagonal pore of **2** using the space filling model (Van der Waals radii). Color scheme: Calcium(II) purple; copper(II), green; isopropyl group of valine residue, yellow gold; nitrogen, light blue; oxygen, red; carbon, grey.

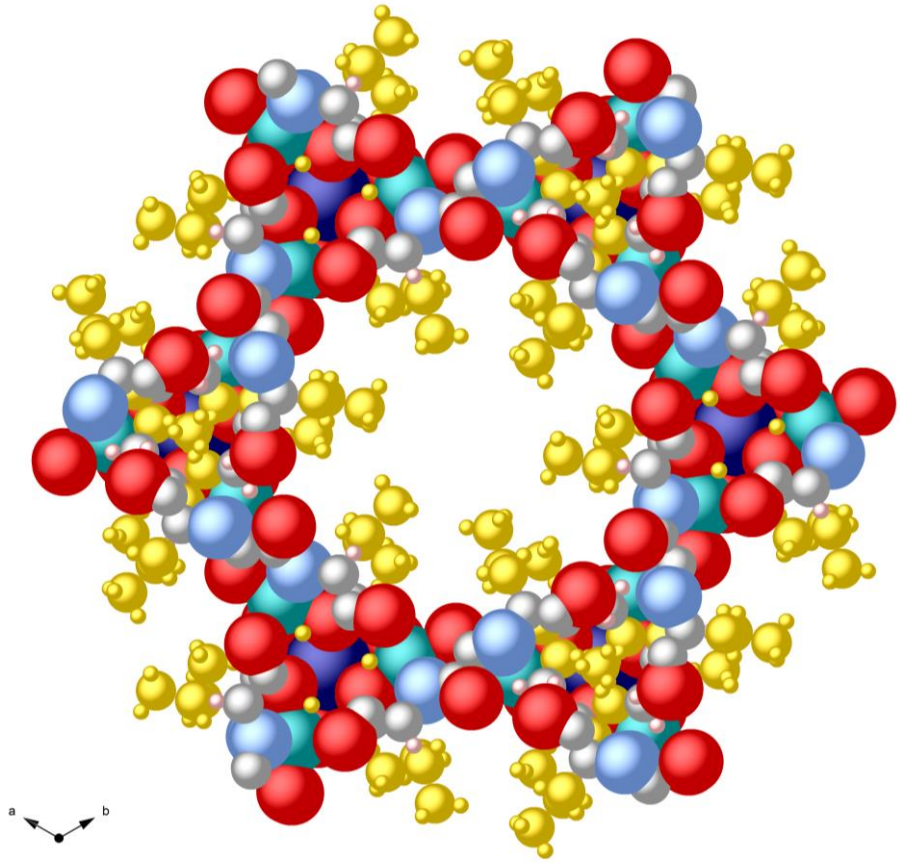

Figure S5. View along the *c* axis of one hexagonal pore of **3** using the space filling model (Van der Waals radii). Color scheme: Calcium(II) purple; copper(II), green; isobutyl group of leucine residue, yellow gold; nitrogen, light blue; oxygen, red; carbon, grey.

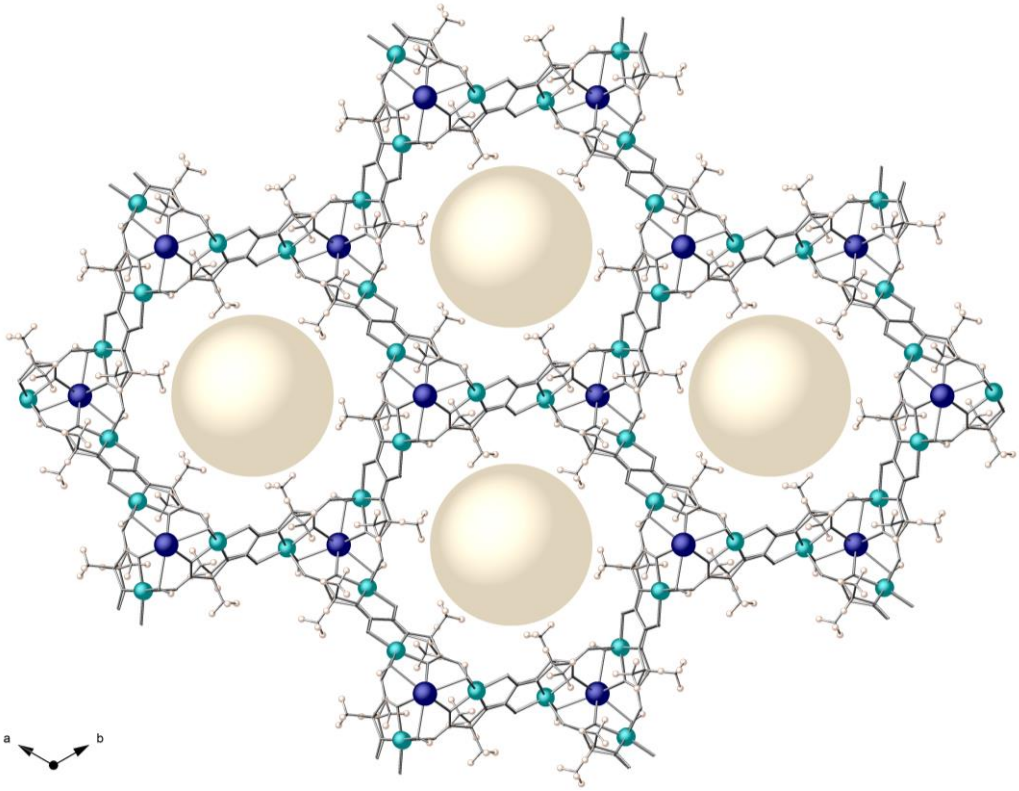

Figure S6. Views along the [001] direction of a portion of the porous X-ray crystal structure of **1**. Pale gold spheres underline the pore size. Free water molecules are omitted for clarity. Color scheme: Calcium(II) purple; copper(II), green; Hydrogen, white; ligands, grey sticks.

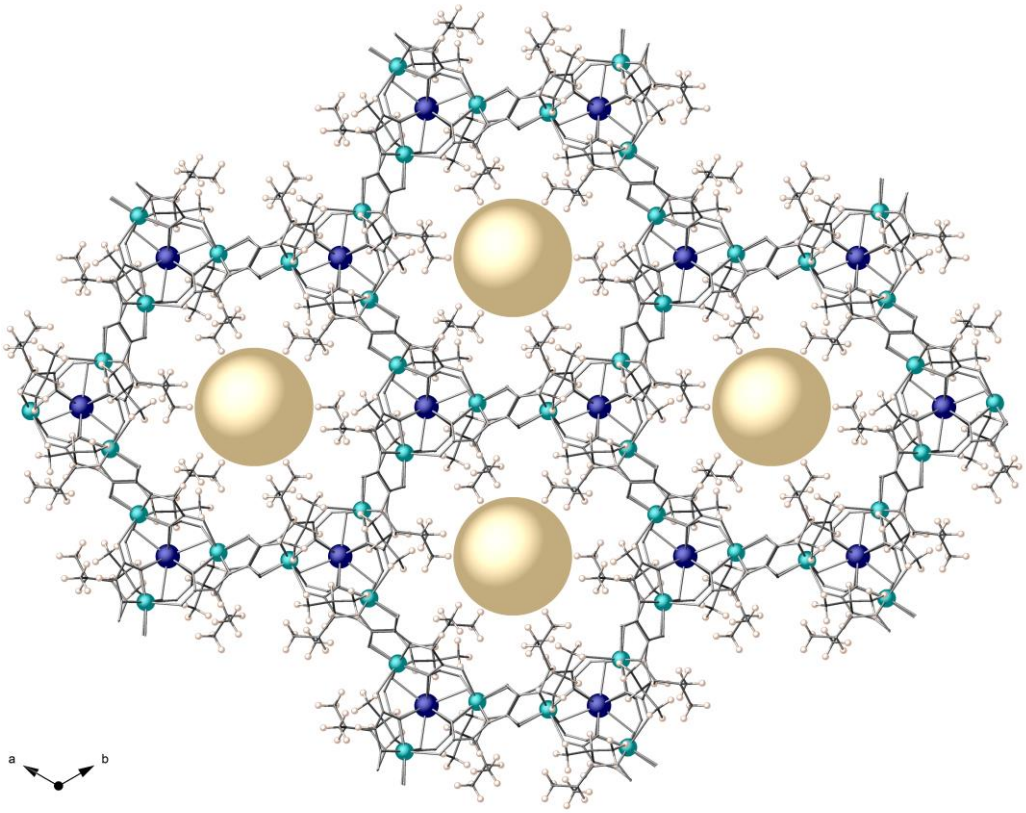

Figure S7. Views along the [001] direction of a portion of the porous X-ray crystal structure of **2**. Gold spheres underline the pore accessible voids. Free water molecules are omitted for clarity. Color scheme: Calcium(II) purple; copper(II), green; Hydrogen, white; ligands, grey sticks.

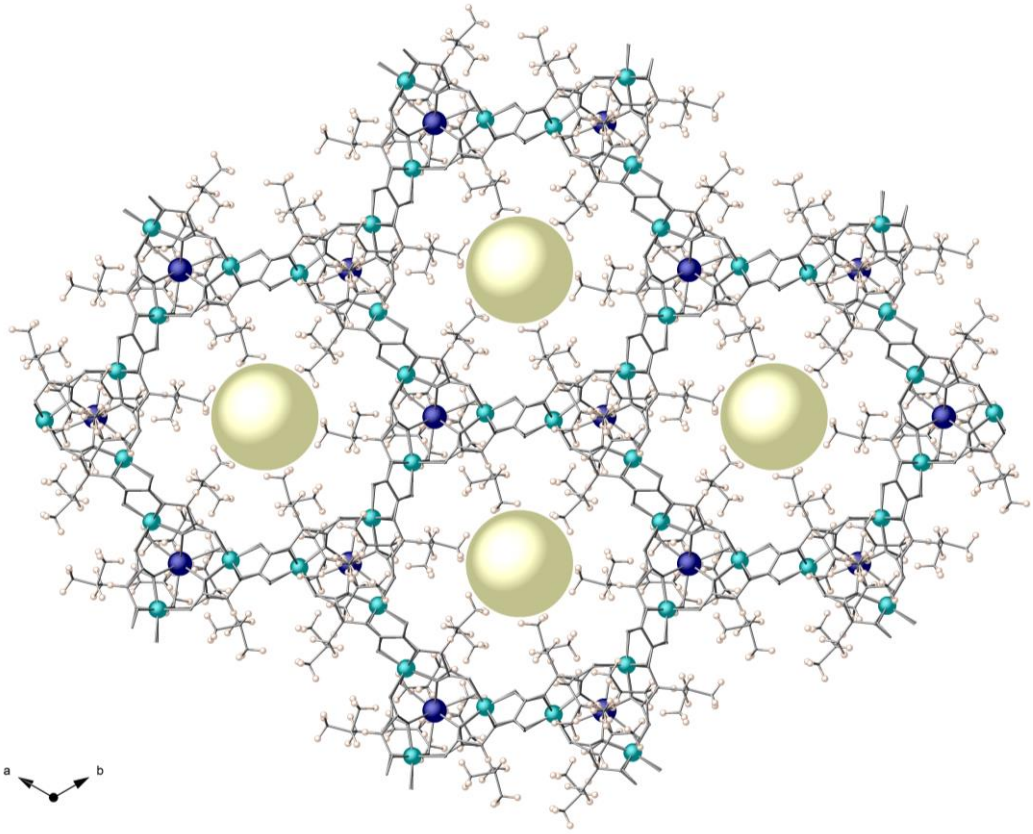

Figure S8. Views along the [001] direction of a portion of the porous X-ray crystal structure of **3**. Pale gold spheres underline the pore accessible voids. Free water molecules are omitted for clarity. Color scheme: Calcium(II) purple; copper(II), green; Hydrogen, white; ligands, grey sticks.

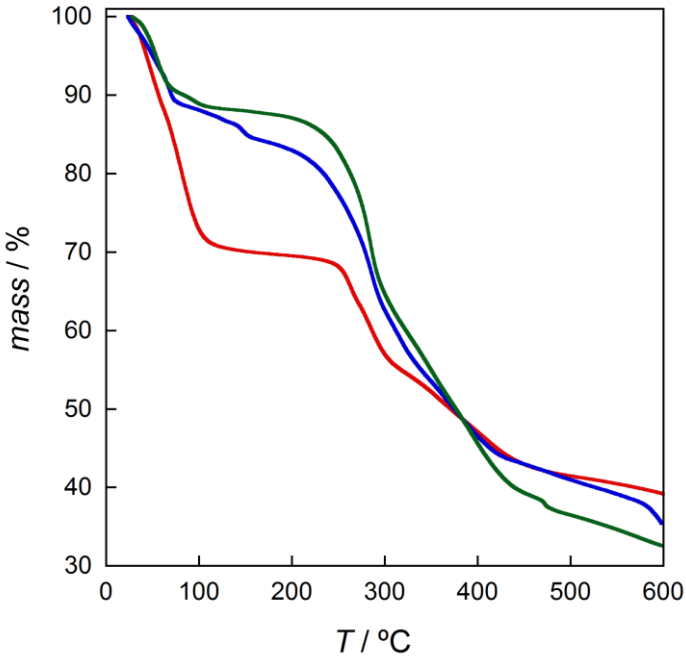

Figure S9. TGA curves for **1** (red), **2** (blue) and **3** (green) under N_2.

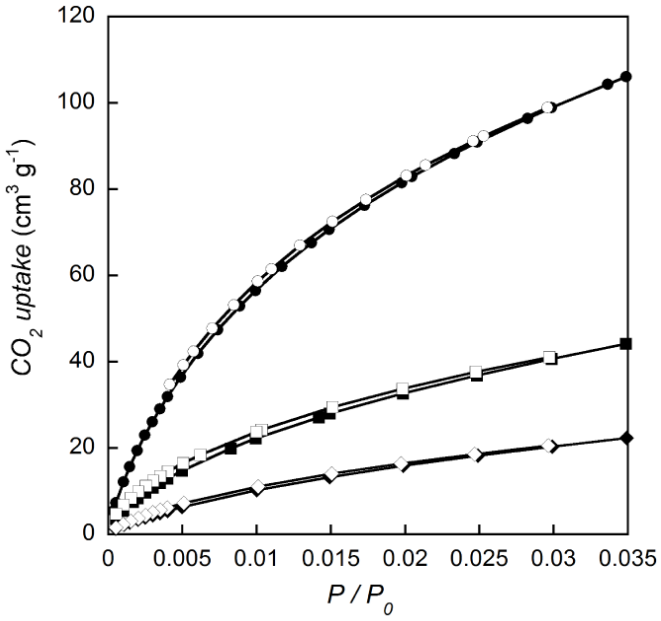

Figure. S10. CO_2 sorption isotherms for the activated compounds **1** (○), **2** (□) and **3** (◊) at 273 K. Filled and empty symbols indicate the adsorption and desorption isotherms respectively.

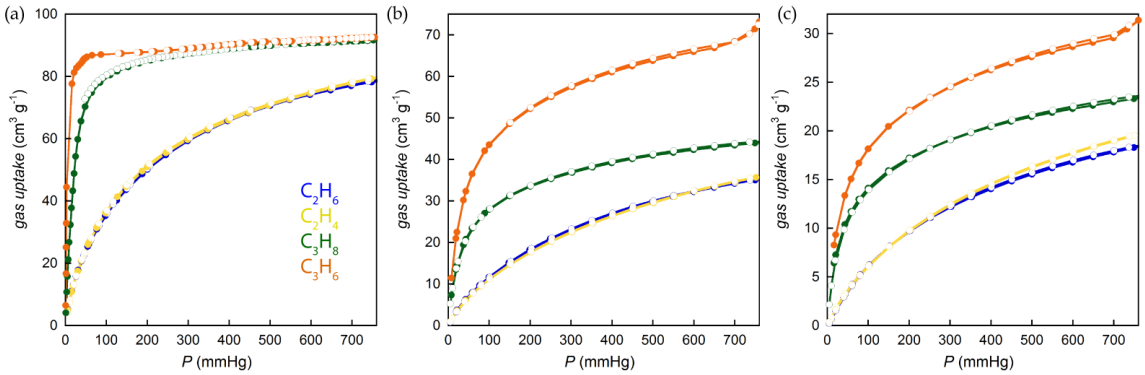

Figure S11. C_2H_6 (blue), C_2H_4 (yellow), C_3H_8 (green) and C_3H_6 (orange) sorption isotherms for the activated compounds **1** (a), **2** (b) and **3** (c) at 273 K.

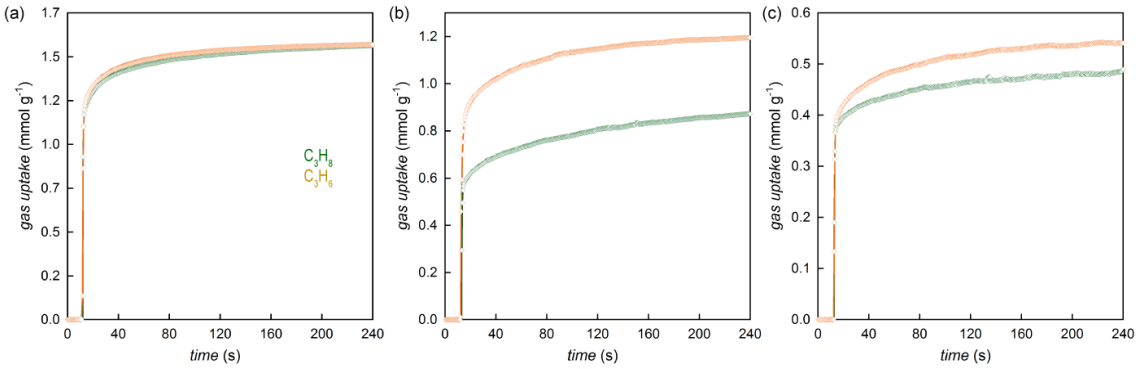

Figure S12. Adsorption kinetic profiles of C_3H_8 (green) and C_3H_6 (orange) for compounds **1** (a), **2** (b) and **3** (c) at 273 K.